

Article

A Pleiotropic Drug Resistance Transporter TaABCG36 Contributes to Defense against *Puccinia triticina* in *Triticum aestivum*

Na Zhang ^{1,†}, Yaya Hu ^{1,2,†}, Yanhui Wu ¹, Johannes Mapuranga ¹ , Ying Yuan ¹ and Wenxiang Yang ^{1,*}

¹ College of Plant Protection, Hebei Agricultural University, Technological Innovation Center for Biological Control of Crop Diseases and Insect Pests of Hebei Province, 2596 Lekai South Street, Baoding 071001, China

² Institute of Cereal and Oil Crops, Hebei Academy of Agriculture and Forestry Sciences, The Key Laboratory of Crop Genetics and Breeding of Hebei, Shijiazhuang 050035, China

* Correspondence: wenxiangyang2003@163.com

† These authors contributed equally to this work.

Abstract: ABC transporters play important roles in plant growth and resistance to abiotic and biotic stresses. Here, we showed that the *TaABCG36* gene positively regulates leaf rust resistance in the wheat line Thatcher + Lr19 (TcLr19) when challenged with an avirulent pathotype of *Puccinia triticina* (*Pt*). The *TaABCG36* gene was cloned from genomic DNA and cDNA from wheat line TcLr19. The clone was 6730 bp in gDNA and 4365 bp in cDNA for this gene. It encoded an ABC transporter with 1454 amino acids in length. BLASTp analysis indicated a considerable identity ABC transporter G family member 36 with *Aegilops tauschii* subsp. *strangulata*, *Triticum dicoccoides*, and *T. aestivum*; thus, we named the gene *TaABCG36*. *TaABCG36* was proved to be a plasma transmembrane protein by bioinformatic analysis and subcellular localization of the *TaABCG36*–GFP fusion protein. The expression of *TaABCG36* in wheat leaves reached a peak at 72 h post-inoculation by *Pt* avirulence pathotype, and the expression was also induced by phytohormone treatments of salicylic acid (SA), abscisic acid (ABA), and methyl jasmonate (MeJA). Three fragments (V1–V3) of the *TaABCG36* gene were introduced to the BSMV-VIGS vector and, thus, silenced the expression of *TaABCG36* in the wheat line TcLr19. All the three BSMV:VIGS-infected plants showed reaction type “3” to *Pt* pathotype THTS, which was fully avirulent on TcLr19 (infection type “0”). Histopathological observation showed that silencing of *TaABCG36* facilitated the formation of haustorial mother cells (HMC) and mycelial growth, implying that *TaABCG36* plays a positive role in the response of TcLr19 against THTS. These results provide molecular insight into the interaction between *Pt* and its wheat host and identify a potential target for engineering resistance in wheat to damaging pathogen of *Pt*.

Keywords: wheat leaf rust disease; *Puccinia triticina*; ABC transporter; *TaABCG36*; virus-induced gene silencing; histopathological observation



Citation: Zhang, N.; Hu, Y.; Wu, Y.; Mapuranga, J.; Yuan, Y.; Yang, W. A Pleiotropic Drug Resistance Transporter TaABCG36 Contributes to Defense against *Puccinia triticina* in *Triticum aestivum*. *Agronomy* **2023**, *13*, 607. <https://doi.org/10.3390/agronomy13020607>

Academic Editors: Ana P. G. C. Marques, Nadia Massa and Santa Olga Cacciola

Received: 4 January 2023

Revised: 6 February 2023

Accepted: 14 February 2023

Published: 20 February 2023



Copyright: © 2023 by the authors. Licensee MDPI, Basel, Switzerland. This article is an open access article distributed under the terms and conditions of the Creative Commons Attribution (CC BY) license (<https://creativecommons.org/licenses/by/4.0/>).

1. Introduction

The ATP-binding cassette (ABC) protein is one of the largest known superfamilies in plants [1]. The ABC proteins are classified into eight subfamilies (ABCA–ABCG, ABCI), with ABCG subfamily being the largest [2]. The full-size ABC transporters consist of two nucleotide-binding domains (NBDs) and two transmembrane domains (TMDs) based on structural features [3] which are considered to play a key role in substrate translocation across the membrane, as well as a hydrophilic nucleotide-binding domain (NBD) that hydrolyses ATP [4].

The first plant ABC transporter was cloned from *Arabidopsis thaliana* [5]; it has now been reported in *Oryza sativa* [6], *Solanum lycopersicum* [7], *Vitis vinifera* [8], strawberry (*Fragaria × ananassa* Duch.) [9], and pineapple (*Ananas comosus* (L.) Merr.) [10]. Plant ABC transporter, especially the ABCG subfamily, is involved in a series of biological functions

including the transport of secondary metabolites [11], heavy metal ions [12], flavonoids [13], and apocarotenoids [14], and it is also involved in the plant response to abiotic and biotic stress [15–17]. ABCG subfamily genes of *A. thaliana* showed seven separated groups on a phylogenetic tree of homologs from a broad range of organisms, with each group comprising multiple genes with similar physiological functions [5]. Full-size ABCGs in plants and oomycetes might have co-evolved in an evolutionary arms race in host plants and their pathogens [18]. NpPDR1 has been shown to be up-regulated by sclareol, an anti-fungal diterpene produced in tobacco leaves [19]. Sclareol has been shown to be transported by NpPDR1 from *Nicotiana plumbaginifolia*, which has been demonstrated to be involved in pathogen resistance. NpPDR1-silenced plants have been proved to more susceptible to *Botrytis cinerea* and *Phytophthora nicotianae* [20]. Similarly, NtPDR1 [21] and NbABCG1/2 [22] transporters from *N. tabacum* and *N. benthamiana*, respectively, are also involved in the secretion of an antimicrobial sesquiterpenoid named capsidiol. Multiple host factors, including AtPDR12 and its homolog NtPDR1, are involved in the function of sclareol-related compounds in resistance against bacterial wilt disease in *Arabidopsis* plants and tobacco [23]. NaPDR1 and NaPDR1-like factors were strongly induced in *N. attenuata* leaves after *Alternaria alternata* inoculation, co-silenced *N. attenuata* plants with NaPDR1 and NaPDR1-like genes showed a high susceptibility to the fungus *A. alternata* than silencing the gene individually, and the transcripts of both genes elicited by the fungus are partially dependent on ethylene and jasmonate signaling [24]. Evidence also suggests that PENETRATION (PEN) 3 (PDR8 or ABCG36) is required for *Arabidopsis* non-host resistance [25].

TaPDR1, which is highly expressed in spike induced by DON (deoxynivalenol) of *cv.* Wangshuibai, has been proved to be related to wheat resistance to *Fusarium graminearum* [26]. *TaABCG2-6* were found to enhance wheat resistance to *Fusarium* head blight [27]. A novel PDR gene *TaPDR7* was found to serve a vital role in the response of wheat to *F. graminearum* [28]. A wheat MRP transporter *TaABCC3* was shown to be involved in grain formation and conferring resistance against mycotoxin secreted by *Fusarium* [29]. *TaMRP1* serves an important role in the glutathione-mediated detoxification [30]. Eighteen wheat ABCG-multi-drug-resistance-associated proteins (MRP) that have uniform distribution with sub-families from rice and *Arabidopsis* were also identified [31]. Another study identified 30 ABC genes in dwarf polish wheat that were characterized and classified into seven sub-families (ABCA–ABCG). The expression of these ABC transporters suggested that they play important roles in metal transport and detoxification [32]. The encoded *LR34res* ABC transporter is essential in modifying the accumulation of 1-*O-p*-coumaroyl-3-*O*-feruloylglycerol, leading to the increased accumulation of antifungal metabolites, essentially priming the wheat for defense [33].

Wheat (*Triticum aestivum* L.) leaf rust disease, which is caused by *Puccinia triticina* (*Pt*), is one of the main serious diseases that results in significant yield and economic losses to wheat production all over the world. Leaf rust resistance gene *Lr19* is among the wheat genes that effectively confer leaf rust resistance. *Lr19* was transferred from the wild relative *Thinopyrum ponticum* into wheat, where it is located on 7DL of the wheat chromosome [34]. In Asia, Canada, Australia, and Europe, the wheat cultivar carrying *Lr19* is still effective against all *Pt* races, and the resistance is expressed throughout the whole growth period and culminates in a hypersensitive response (HR) at the infection site, which is also known as race-specific resistance [35,36]. Though gene *Lr19* is widely effective and has the potential to be deployed in the field worldwide, no thorough investigation has been conducted except for analysis of close neighborhood molecular markers [35,37], analysis of agronomic traits of wheat lines carrying *Lr19* [38,39], resistance-related functional analysis on wheat *TcLr19* plants [40,41], and homologous identification in *Aegilops tauschii*, the wheat wild relatives [42]. A candidate gene *AG15* for *Lr19*, which is 4121 bp cDNA in length, had been cloned [43], but little is known about the resistant mechanism. More related genes that may participate in the resistance reaction of *Lr19* should be cloned to further study the resistance mechanism of this gene.

We constructed an EST library of TcLr19 challenged with the *Pt* pathotype THTS; 472 unisequences were acquired from 649 high-quantity ESTs. Of those high-quantity ESTs, 18.4% were annotated as being related to energy and metabolism, 20.8% were classified as disease-resistance- and signal-transduction-related, and 7.2% were annotated as transporter genes. The fact that the transporters comprise a relatively high proportion in the expressed library indicated that the expressed transporters (PDRs for example) may be involved in wheat resistance to the parasitic fungal pathogen *Pt*. A specific fragment of 447 bp, which showed high similarity with PDR members following blast, was selected as the target. In this study, *TaABCG36* was cloned based on the target fragment, and its roles in wheat resistance were tested via the virus-induced gene silencing (VIGS) technique. Transcriptional levels of this gene in wheat line TcLr19 treated with salicylic acid (SA), abscisic acid (ABA), and methyl jasmonate (MeJA) were also investigated to explore the resistance signal pathway *TaABCG36* may involve.

2. Materials and Methods

2.1. Plant Materials, *Pt* Pathotype, and Primers

Wheat near isogenic line TcLr19 and Thatcher were employed as the plant materials. Thatcher is a line that is susceptible to all *Pt* pathotypes. TcLr19, with a Thatcher background, carries leaf-rust-resistance gene *Lr19* and is effective against all *Pt* pathotypes in China. The plant materials were provided by International Maize and Wheat Improvement Center (CIMMYT) and bred and stored in Hebei Agricultural University (HAU). When the experiment was carried out, the seedlings were planted in the greenhouse in HAU, Baoding, China. *Pt* pathotype 09-12-284-1 (THTS), the avirulence/virulence of this pathotype, was identified according to the infection type (IT) in a series of near-isogenic lines (NILs) of wheat leaf rust (*Lr*) resistance gene in Thatcher background and named according to Long and Kolmer [44]. All primers used in this study are listed in Table 1.

Table 1. Primers used for cloning, qRT-PCR, vector construction, and gene silencing.

Primers	Primer Sequence (5'-3')	Primer Application
3'-GSP1	CAAGAGCAAGAGCCATCCAGCAGC	RACE amplification
5'-GSP2	AGCTCCTTCTTATAGCTCTCCCGGTGT	
ABCG-F	ATGGACGCGACGGCGGAAATCCAC	Full length amplification
ABCG-R	CATTCCGGTGGTGCAAAAATGT	
GAPDH-F	AACTGCCTTGCTCCTCTTG	Real-time quantitative PCR
GAPDH-R	CATCAAACCCTCAACAATGC	
qABCG-F	TTCGATGACATCATCCTCCT	
qABCG-R	GCACCCAGTATTGCTTTTGA	
V-ABCG-F1	ATATTAATTAATTCGATGACATCATCCTCCT	
V-ABCG-R1	TATGCGGCCGCGCACCCAGTATTGCTTTTGA	
V-ABCG-F2	ATATTAATTAAGAAAGATGCATTGGTTGGTC	Virus-induced gene silencing
V-ABCG-R2	TATGCGGCCGCTCGTGCAAACCCACAGTTCTA	
V-ABCG-F3	ATATTAATTAACAACACTGGTGAGATGCTGGT	
V-ABCG-R3	TATGCGGCCGAGGAGGATGATGTCATCGAA	Subcellular localization
Y-ABCG-F	GCTCTAGAATGCCGACGATCGAGGTGCGGTTCG	
Y-ABCG-R	TCCCCGGGTACCTCTTCTGGAAGTTGAGCTTCA	

2.2. *Pt* and Phytohormone Treatments

A single spore isolate of *Pt* pathotype THTS was used for seedling inoculation. *Pt* inoculation was performed as per the method outlined by Li et al. [41]. MeJA (1 mM) and ABA (1 mM) (www.sigmaldrich.com, accessed on 28 July 2022) and SA (5 mM) (www.sangon.com, accessed on 28 July 2022) were sprayed directly on the 12-day-old TcLr19 seedling leaves (2-leave stage). After *Pt* inoculation or treatment with phytohormones, plants were kept in a moist chamber with 100% relative humidity (RH) for 16 h in the dark and then transferred to a greenhouse compartment kept at 18–22 °C with a 16 h photoperiod and 80% RH. The treated leaves were harvested after 0, 6, 12, 18, 24, 36, 48, 72,

96, 144, 216, and 288 h. Seedlings sprayed with distilled water were used as control, with three replicates for each.

2.3. Genomic DNA, RNA Extraction, and cDNA Synthesis

Genomic DNA of TcLr19 was extracted by the CTAB method. Total RNAs of different treatments of the three replications were extracted according to the BIOZOL Total RNA Extraction Reagent (BioFlux, Suzhou, China) handbook. cDNA was synthesized using Reverse Transcriptase M-MLV (RNase H⁻) (TaKaRa, Kusatsu, Japan). The synthesized cDNA samples were stored at -20 °C before use.

2.4. Isolation and Characterization of TaABCG36

The fragment of 447 bp, which was induced in *Pt*-inoculated TcLr19, was selected as the target sequence; 5'- and 3'- was amplified according to the user manual of SMARTerTM RACE cDNA Amplification Kit (Clontech, Mountain View, CA, USA). The full length of the *TaABCG36* gene was amplified with cDNA and gDNA of TcLr19 as the template by ABCG-F/ABCG-R (Table 1). The purified PCR products were linked into the pGEM-T vector (Promega, Madison, WI, USA). Positive recombinant plasmids were sequenced by Sangon Biotech (Shanghai, China) Co., Ltd.

Sequences from 5'- and 3'-amplicons were assembled using DNAMAN software. Sequence analysis was performed on <http://www.ncbi.nlm.nih.gov>, accessed on 28 July 2022. Chromosomal location was analyzed on <http://www.wheatgenome.org/>, accessed on 28 July 2022. The conserved domains were deduced using InterProScan (<http://www.ebi.ac.uk/interpro/search/sequence/>, accessed on 28 July 2022). TMpred (http://www.ch.embnet.org/software/TMPRED_form.html, accessed on 28 July 2022) was used for the prediction of the transmembrane region. The phylogenetic tree was generated by MEGA X software (<https://www.megasoftware.net/> accessed date 28 July 2022).

2.5. Quantitative Real-Time PCR

The partial coding region of 108 bp from *TaABCG36* was amplified using the gene-specific primers qABCG-F and qABCG-R (Table 1). The wheat *GAPDH* gene, which was amplified with the forward primer GAPDH-F and the reverse primer GAPDH-R (Table 1), was utilized to amplify an internal control to normalize the RT-PCR results. For a negative control, a reaction mix without reverse transcriptase was used as a template in the reaction. The relative expression level of the target gene was presented as fold change compared with the internal control using the 2^{-Δct} method, and data were analyzed with DUNCAN's multiple range test ($p < 0.05$). Three biological replications were performed for each test.

2.6. Subcellular Localization of TaABCG36

The cDNA fragments containing *TaABCG36* open-reading frame (ORF) were amplified by PCR with the specific primers containing enzyme sites of *Sma* I and *Xba* I (Table 1) and then inserted upstream of the green fluorescent protein (GFP) coding region in the pCaMA:GFP vector. The recombined plasmid of pCaMA:TaABCG36-GFP and pCaMA:GFP was transformed into onion epidermal cells by particle bombardment (Bio-Red), as described by Li et al. [41]. Bombardment was conducted with three replications, and at least 10 individual cells for each bombardment were analyzed. The GFP signal was detected using a confocal microscope (OLYMPUS BX51, Tokyo, Japan).

2.7. BSMV-Mediated TaABCG36 Gene Silencing

Three specific cDNA fragments of 169, 206, and 197 bp in length covering different parts of the coding region were designed for silencing *TaABCG36*. Off-target prediction was followed by si-Fi software [45]. The fragments were amplified using the primer pair V-ABCG-F1-F3/R1-R3 (Table 1, and then reversely inserted respectively into the BSMV:γ vector to form the recombinant vector BSMV:γTaABCG36as1-3, following the method of Zhang et al. [46]. Equal quantities of BSMV:TaABCG36as, BSMV:α, and BSMV:β were

used to inoculate the third fully expanded wheat seedling leaves, with BSMV:TaPDSas and BSMV:γ as the controls. Seedlings of TcLr19 and Thatcher that were not pre-infected by BSMV were mock-inoculated with 1 × GPK buffer (0.1 M glycine, 0.06 M K₂HPO₄, 1% tetrasodium pyrophosphate, 1% bentonite and 1% celite, pH 8.5). The fourth wheat leaves were further treated with *Pt* pathotype THTS 12 d after virus inoculation. At least 14 plants were subjected to silencing for each of the VIGS construct, with three replications. The leaves were sampled at 24, 48, and 120 hpi with *Pt* for histopathological observation. Three independent sets of inoculations were performed.

2.8. Histopathological Observations of Fungal Growth and Host Response

For all microscopic observations, five 3-cm leaf pieces from the central portion of wheat leaf inoculated with BSMV, BSMV:TaABCG36as1-3 were collected at time intervals of 24, 48, and 120 hpi. After the leaf tissue was cut, all specimens were stained, as described by Li et al. [41]. For confocal microscopy and haustorial observation, specimens were observed using an Olympus FV 1000 confocal microscope (Olympus, Tokyo, Japan) under 405 and 488 nm lasers at 40× magnification, as described by Wang [47]. At least 20 infection sites were examined, and at least 60 infection sites in 5 randomly selected leaf segments were evaluated for each treatment. Infection types of leaf rust were examined 14 d after inoculation.

3. Results

3.1. Isolation and Characterization of TaABCG36

For the gene cloning from cDNA, a 3'-product of 3481 bp in length was amplified using 3'-GSP1 primers and comprised 181 bp overlapping sequences with the target 447 bp sequence. The 5'-RACE PCR product was 1160 bp in length, with 281 bp overlapping sequences. The assembled sequence indicated a 5'-UTR of 347 bp, 3'-UTR of 294 bp, and a 33 bp poly(A) tail. Then, the *TaABCG36* gene from cDNA and gDNA was cloned from TcLr19 with full-length primers designed based on the deduced ORF sequence (Figure S1). Sequence analysis showed there were 20 introns in the 6730 bp cloned from gDNA, resulting in an ORF of 4365 bp. Based on blast searches of IWGSC RefSeq v1.0 (bread wheat), the gene was located on wheat chromosomes 3A, 3B, and 3D, with three copies. It encoded a predicted protein with 1454 amino acids (aa), with a predicted molecular mass of 163.38 kDa and a calculated pI of 7.27. According to SMART gene structure analysis, the protein sequence contains two TMD domains in the order of NBD₁-TMD₁-NBD₂-TMD₂ that have a reverse-domain organization, with the nucleotide-binding domain preceding the transmembrane domain. The two ABC domains were composed of 226 aa and 193 aa, respectively, and thirteen transmembrane segments. Each ABC domain with a well-conserved Walker A motif (GPPGSGKTT or GVSGAGKTT), a less-conserved Walker B (ALFMDE or IIFMDE), and a Walker C (GISGGQRKRVTTGEML or GLSTEQRKRLTIAVEL) (Figure S2). Based on all the structural conservation, the protein was confirmed to be a member of the full-length size pleiotropic drug resistance (PDR) family.

The phylogenetic tree was constructed based on the deduced TaABCG36 protein and homologous amino acid sequences of ABC family members downloaded from the NCBI database, and it showed that the protein had a high similarity (99.85%, 99.8%, and 99.65%, respectively) to that of the ABC transporter G family member 36 (ABCG36) from *Aegilops tauschii* subsp. *strangluata* (XP_020180656.1), ABCG36 from *T. aestivum* (XP_044349050.1), and *T. dicoccoides* (XP_037413166.1) (Figure 1); thus, we named the acquired protein TaABCG36.

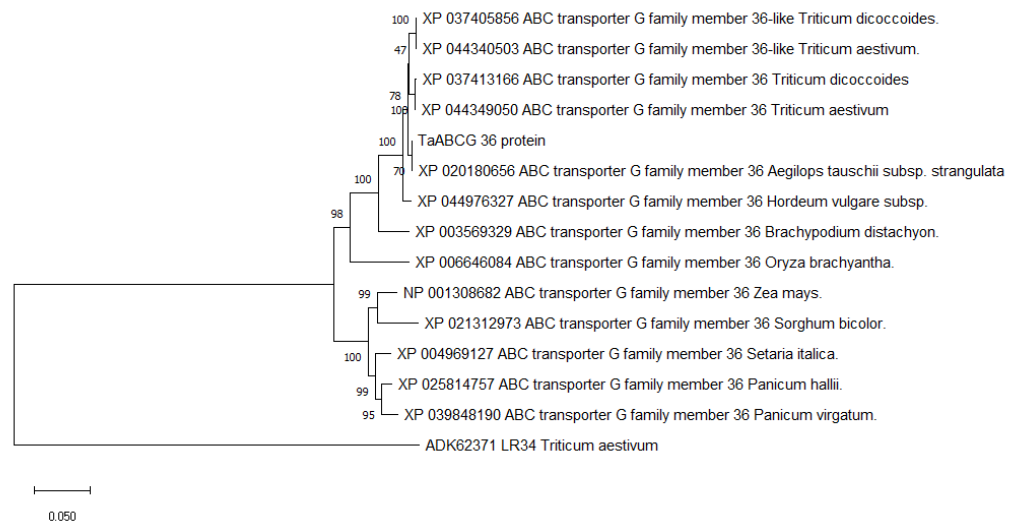


Figure 1. Phylogenetic tree based on the deduced amino acid sequences of TaABCG36 and those downloaded from NCBI.

3.2. Expression Patterns of TaABCG36 in TcLr19

We measured the mRNA level of the *TaABCG36* gene by quantitative real-time PCR (qRT-PCR) with specific primers qABCG-F and qABCG-R (Table 1). Total RNA from TcLr19 treated with *Pt* and phytohormones were used as templates. Under inoculation with the *Pt* pathotype THTS, the transcription of *TaABCG36* increased and reached a peak expression at 72 hpi in TcLr19-*Pt* plants, about six times compared with *TaABCG36* expression under non-inoculation (0 h) (Figure 2A). Markedly increased transcripts were detected in MeJA- and SA-treated plants compared with mock plants before 6 hpi (hours post-inoculation) and showed a similar expression profile (Figure 2B,C). Markedly increased transcripts also detected in ABA-treated plants compared with mock plants before 6 hpi, and this lasted to 72 hpi in ABA-TcLr19 plants, with two transcription peaks at 12 hpi and 36 hpi (Figure 2D). Considering the results above, TaABCG36 may be involved in the resistance of TcLr19 to *Pt*, as well as a signal pathway induced by MeJA, ABA, and SA.

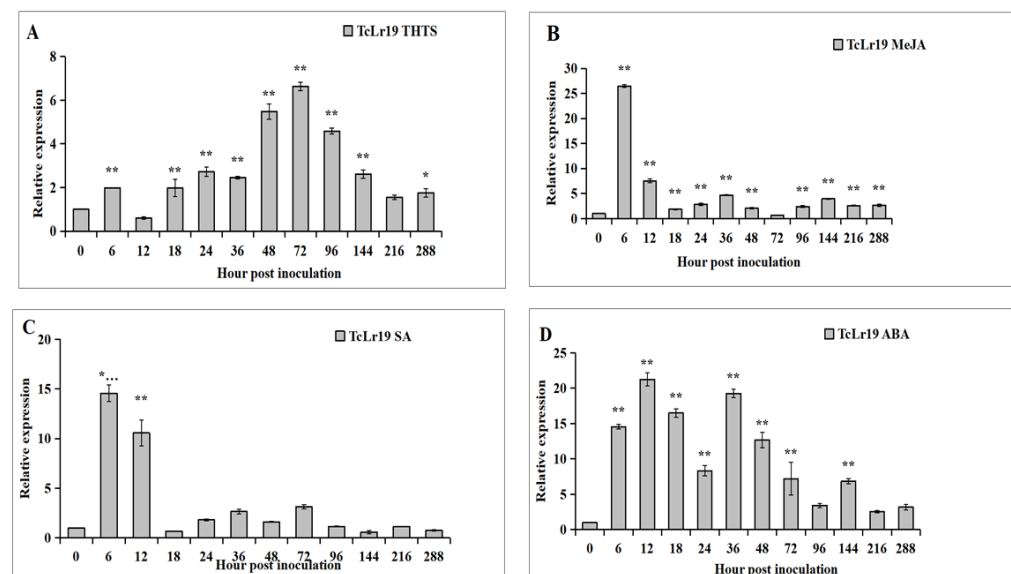


Figure 2. Transcription pattern of *TaABCG36* in TcLr19 treated with THTS (A), MeJA (B), SA (C), and ABA (D). *: $p < 0.05$, **: $p < 0.01$, ***: $p < 0.001$, ($n = 3$).

3.3. *TaABCG36* Is a Plasma-Membrane-Localized Protein

Onion cells were bombarded with constructed recombination vectors with a particle gun and cultured in darkness at 25 °C for 16 h. Fluorescence was observed under 488 nm. The results showed that the pCaMA-GFP vector (control) was expressed in the cell membrane, nucleus, and cytoplasm, that is, green fluorescence was distributed in the whole cell (Figure 3A), whereas the green fluorescence of the pCaMA:TaABCG36-GFP fusion protein was mainly concentrated on the cell membrane (Figure 3B), indicating that TaABCG36 was a plasma-membrane-localized protein, confirming the bioinformatic analysis.

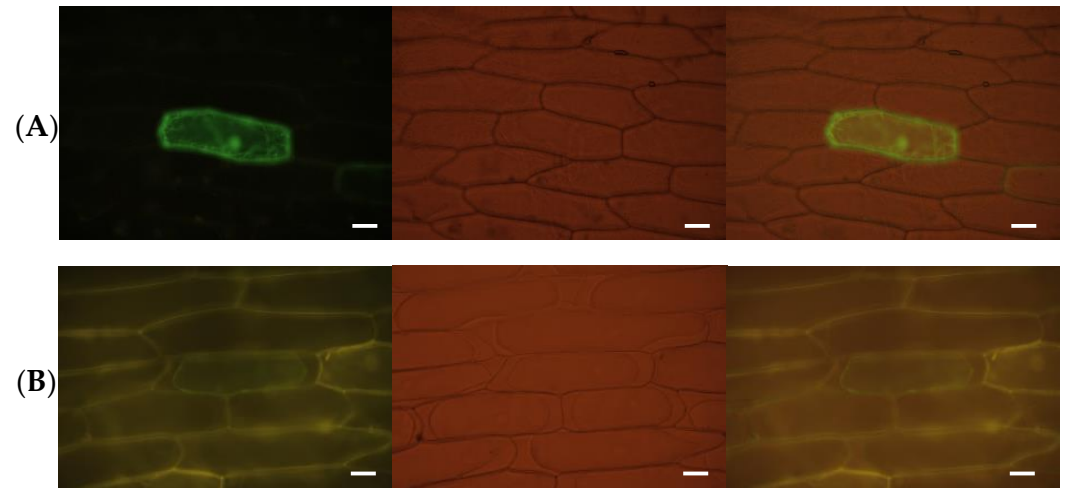


Figure 3. Subcellular localization of the TaABCG36-GFP fusion protein. (A) The control GFP protein. (B) The TaABCG36-GFP fusion protein. Scale bars are 50 μ m.

3.4. *TaABCG36*-Silenced Plants Showed Decreased Leaf Rust Resistance

The three VIGS fragments were all efficient in silencing the target gene by off-target prediction (Table S1). Severe chlorophyll photobleaching observed on the fourth leaves of the BSMV:TaPDS-infected plants indicated that a feasible genetic interference system was operated in this study (Figure 4A). Immune (infection type “0”, with no symptom on the leaves after inoculation with THTS) was shown on TcLr19 and BSMV:00 (Figure 4B,C). A faded stripe appeared on BSMV:00-infected TcLr19 (Figure 4C), indicating that pre-inoculation of the virus had not affected the incompatibility reaction between wheat TcLr19 and *Pt*. Uredinia erupted on the leaves of Thatcher plants at 14 dpi, with infection type “4” (Figure 4D). For the VIGS plants analyzed, 68.3%, 69.3% and 66.0% of plants presented diseased phenotypes, indicating efficient silencing by BSMV:V1, BSMV:V2, and BSMV:V3, respectively (Table S2). On those infected by BSMV:V1-3, IT (infection type) “3” presented in the form of faded spots around the uredinia (Figure 4E–G). Limited uredinia and spore development were observed on leaves treated with BSMV:V2 and BSMV:V3 (Figure 4F,G), indicating that *TaABCG36* was effectively silenced by BSMV:V1, followed by BSMV:V2 and BSMV:V3.

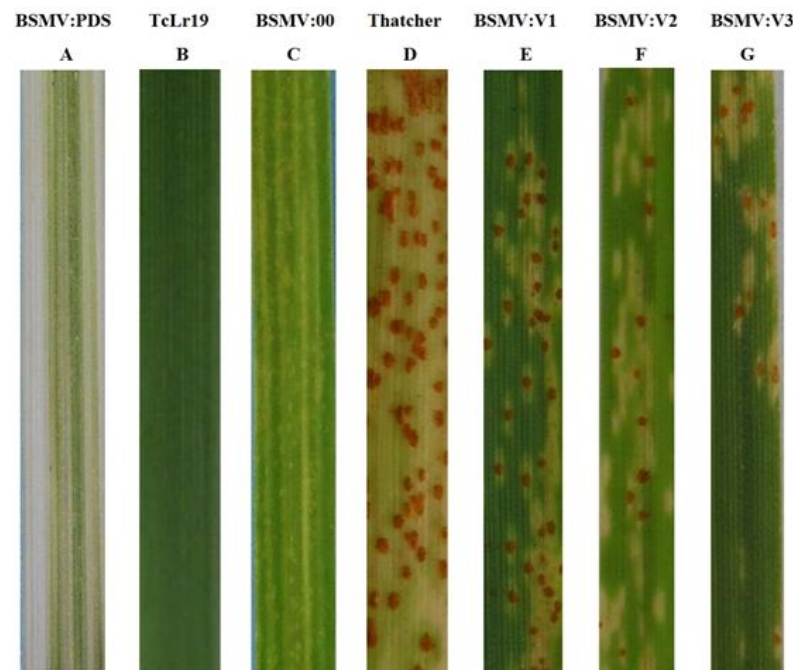


Figure 4. Phenotypic characterization of wheat leaves after virus-induced *TaABCG36*-gene silencing. (A) (BSMV:PDS): TcLr19 infiltrated by BSMV:PDS; (B) (TcLr19): wild type of TcLr19; (C) (BSMV:00): TcLr19 infiltrated by BSMV:00; (D) (Thatcher): the susceptibility line. (E–G) (BSMV:V1–V3): TcLr19 infiltrated by BSMV:V1, BSMV:V2, and BSMV:V3, respectively. All these were inoculated with *Pt* pathotype THTS.

3.5. Histopathological Analysis of *TaABCG36* Knockdown Leaves

The growth of *Pt* in leaves treated with BSMV:V1–3 was examined. Urediospores had germinated and infection structures (appressoria, substomatal vesicles, infection hyphae, and haustorial mother cells) had all formed by 24 hpi in the BSMV:00 pre-inoculated TcLr19 leaves. No visible secondary hyphae formed, whereas necrotic cells formed around haustorial mother cells by 48 h and 120 h (Figure 5A–C), indicating a resistance reaction. Compared to plants inoculated with BSMV:00, no necrotic cells had formed in leaves pre-inoculated with BSMV:V1, BSMV:V2, and BSMV:V3 by 24 hpi (Figure 5D,G,J); slight secondary hyphae and haustoria formed by 48 hpi (Figure 5E,H,K); and hyphal branches had formed by 120 hpi. Necrotic cells formed with hyphae growth (Figure 5F,I,L). In Thatcher plants (susceptible line, no pre-inoculated with BSMV), appressoria, substomatal vesicles, infection hyphae, and haustorial mother cells formed at 24 hpi (Figure 5M); the secondary hyphae formed at 48 hpi (Figure 5N). Additionally, massive secondary hyphae and haustorium formed at 120 hpi (Figure 5O), and no necrotic cells formed during our observations.

These results confirmed that silencing the *TaABCG36* gene resulted in accelerated growth and infection processes by the *Pt* isolate THTS. Combining the results of the histopathological studies and the phenotypic evaluation above clearly indicated that *TaABCG36* acts as a positive regulator for leaf rust resistance in the wheat line TcLr19 responding to *Pt*.

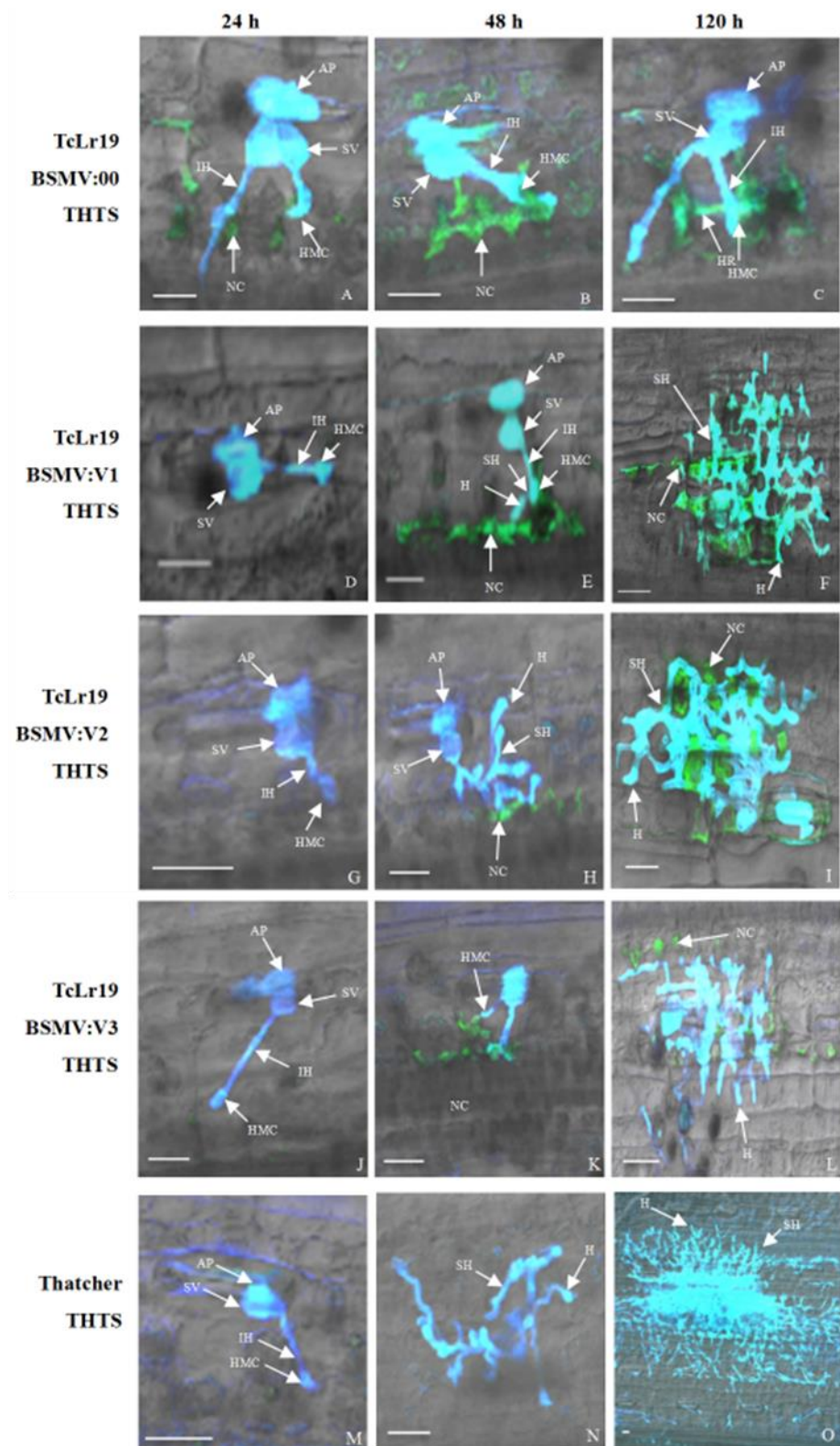


Figure 5. Histopathological observation of BSMV-infiltrated TcLr19 wheat leaves at 24 h, 48 h, and 120 h after inoculation with THTS. (A–C): TcLr19 infiltrated by BSMV:00 inoculation with THTS; (D–L): TcLr19 infiltrated by BSMV:V1–3 and inoculation with THTS; (M–O): Thatcher after inoculation with THTS; AP: appressorium; IH: infection hypha; SV: substomatal vesicle; HMC: haustorial mother cell; SH: second hypha; H: haustorium; NC: necrotic cell. Scale bars are 30 μ m.

4. Discussion

Considerable research has been conducted to identify genes in wheat that are involved in resistance to *Pt* or other biotic responses [48,49], such that further engineering of these genes can occur with the aim of improving disease control. Members of the ABC transporter family have received much attention, as they play important roles in various biological processes associated with defense against pathogens [19–28].

In this study, we focused on ABCG which was induced by *Pt* infection. Subcellular localization by the bioinformatic and transient expression system both indicated that TaABCG36 is a protein located in the plasma membrane, where it may export substrates synthesized in the cell or excrete xenobiotic compounds entering the cell. Identification of the transported substrates is often complicated by their pleiotropic effects, and reports on purified and biochemically analyzed proteins are still rare. Sclareol, an antifungal diterpene, is thought to be excreted by NpPDR1 in *N. plumbaginifolia* and SpPDR (SpTUR2) in *S. polyrrhiza* [20,50] and plays a critical role for PDR transporters.

The strong association with lipid metabolism suggests that certain lipids might directly serve as transport substrates of the ABC transporter. Numerous ABC transporters have been reported to play roles in the rearrangement of certain lipids within the membrane bilayer in various organisms. For example, PDR5 from *Saccharomyces cerevisiae* was characterized as a phosphatidylethanol amine (PE) floppase in addition to its function in extruding a diverse set of cytotoxic compounds [51]. A half-size ABCG transporter from *Leishmania* (a human pathogen) is responsible for the exposure of phosphatidylserine (PS) on its plasma membrane (PM) [52]. *Lr34*, a wheat ABC transporter which confers resistance to the leaf rust pathogen, promoted oil body formation in a mutant defective in PL transfer in the secretory pathway when heterologously expressed in *S. cerevisiae* [53]. Further studies will be conducted to verify the potential substrates involved in wheat resistance to *Pt*.

The transcription profile showed that the expression of TaABCG36 was low under normal conditions but increased in response to *Pt* infection and induction of the phytohormones ABA, SA, MeJA at certain time points with differences. It also revealed that the expression of TaABCG36 is distinctly regulated by biotic and phytohormone stress. The decreased expression suggested that TaABCG36 may excrete toxic compounds to protect the plant itself from pathogen invasion, and its substance may be harmful to plant cells when accumulated in the tissue [1].

Virus-induced gene silencing was used to study the function of TaABCG36 in the wheat–*Pt* interaction system. Our results showed that VIGS knockdown decreased resistance of TcLr19 to *Pt*. Histopathological observations showed that massive secondary hyphae of the *Pt* formed when inoculated with pathotype THTS, which is avirulent on TcLr19, in TaABCG36-silenced TcLr19 plants. These results showed that our newly named gene TaABCG36 plays a positive role in the interaction between wheat and *Pt*.

A study of the *Pt* infection process has shown that germ tubes began to form 6 h post-inoculation, then the primary hyphae began to grow 12 hpi. However, appressorium, substomatal vesicles, primary hyphae, and haustorial mother cells were formed during the critical moment (12–24 h) [54] (Figure 5A,D,G,J,M). In incompatible interactions, necrotic cells presented around haustorial mother cells at 24 hpi, and the growth of haustorial mother cells was inhibited. Haustorial mother cells stopped growing at 48 h (Figure 5B). In the incompatible interaction (Figure 2A), TaABCG36 showed peak expression at 72 hpi, which was higher than mock inoculation. Combining with qRT-PCR and histopathological observation, TaABCG36 may play roles in inhibiting HMC formulation. Haustorium is a key structure for secreted effectors, which act as key factors for virulence or avirulence for parasitic pathogens of *Pt*. We can deduce that a molecule secreted from haustorium functions as a potential substrate for the TaABCG36 transporter. Furthermore, transcription regulation, as well as the transportation substrate of TaABCG36, should be studied to clarify the molecular mechanism of TaABCG36 contribution to *Lr19*-mediated resistance.

5. Conclusions

A pleiotropic drug resistance (PDR)-type transporter, *TaABCG36*, was cloned from wheat line TcLr19; the gene was induced by *Puccinia triticina* and phytohormone (SA, MeJA, and ABA). The *TaABCG36* gene plays a positive role in the response of TcLr19 against *Pt* pathotype THTS.

Supplementary Materials: The following supporting information can be downloaded at: <https://www.mdpi.com/article/10.3390/agronomy13020607/s1>, Figure S1. PCR amplicons of 3'RACE (A), 5'RACE (B), and in gDNA and cDNA (C) of *TaABCG36* from wheat TcLr19. M1: DL2000 marker, M_λ: λDNA/HindIII Marker. Figure S2. Analysis of nucleotide and predicted amino acid sequences of *TaABCG36* nucleotide-binding domains are shown in grey. Walker A, Walker B, and Walker C are boxed. Transmembrane segments are underlined. Silence sites of V1 (yellow), V2 (blue), and V3 (green) are highlighted. Table S1. Off-target prediction of the three BSMV fragments by si-Fi software. Table S2. Statistical analysis of the VIGS TcLr19 plants.

Author Contributions: Writing—first draft preparation, N.Z. and Y.H.; writing—review and editing, Y.W. and J.M.; figures and tables, Y.H., Y.Y. and Y.W.; funding acquisition, W.Y. and N.Z. All authors have read and agreed to the published version of the manuscript.

Funding: This work was funded by the National Science Foundation of China (32172367) and the Natural Science Foundation of Hebei Province (C2021204055).

Data Availability Statement: Not applicable.

Acknowledgments: The authors would like to thank Xianming Chen (Washington State University, USA) for providing the BSMV silencing vector and Zhiying Ma (Hebei Agricultural University, China) for providing the vector of subcellular localization.

Conflicts of Interest: The authors declare no conflict of interest.

References

1. Rea, P.A. Plant ATP-binding cassette transporters. *Annu. Rev. Plant Biol.* **2007**, *58*, 347–375. [[CrossRef](#)] [[PubMed](#)]
2. Kang, J.; Park, J.; Choi, H.; Burla, B.; Kretzschmar, T.; Lee, Y.; Martinoia, E. Plant ABC transporters. *Arab. Book/Am. Soc. Plant Biol.* **2011**, *9*, e0153. [[CrossRef](#)] [[PubMed](#)]
3. Hollenstein, K.; Frei, D.C.; Locher, K.P. Structure of an ABC transporter in complex with its binding protein. *Nature* **2007**, *446*, 213–216. [[CrossRef](#)] [[PubMed](#)]
4. Locher, K.P. Structure and mechanism of ABC transporters. *Curr. Opin. Struct. Biol.* **2004**, *14*, 426–431. [[CrossRef](#)]
5. Dudler, R.; Hertig, C. Structure of an MDR-like gene from *Arabidopsis thaliana*: Evolutionary implications. *J. Biol. Chem.* **1992**, *267*, 5882–5888. [[CrossRef](#)]
6. Garcia, O.; Bouige, P.; Forestier, C.; Dassa, E. Inventory and comparative analysis of rice and *Arabidopsis* ATP-binding cassette (ABC) systems. *J. Mol. Biol.* **2004**, *343*, 249–265. [[CrossRef](#)]
7. Ofori, P.A.; Mizuno, A.; Suzuki, M.; Martinoia, E.; Reuscher, S.; Aoki, K.; Shibata, D.; Otagaki, S.; Matsumoto, S.; Shiratake, K. Genome-wide analysis of ATP-binding cassette (ABC) transporters in tomato. *PLoS ONE* **2018**, *13*, e0200854. [[CrossRef](#)]
8. Cakir, B.; Kilickaya, O. Whole-genome survey of the putative ATP-binding cassette transporter family genes in *Vitis vinifera*. *PLoS ONE* **2013**, *8*, e78860. [[CrossRef](#)]
9. Shi, M.Y.; Wang, S.S.; Zhang, Y.; Wang, S.; Zhao, J.; Feng, H.; Sun, P.P.; Fang, C.B.; Xie, X.B. Genome-wide characterization and expression analysis of ATP-binding cassette (ABC) transporters in strawberry reveal the role of FvABCC11 in cadmium tolerance. *Sci. Hortic.* **2020**, *271*, 109464. [[CrossRef](#)]
10. Chen, P.J.; Li, Y.; Zhao, L.H.; Hou, Z.M.; Yan, M.K.; Hu, B.Y.; Liu, Y.H.; Azam, S.M.; Zhang, Z.Y.; Rahman, Z.; et al. Genome-wide identification and expression profiling of ATP-binding cassette (ABC) transporter gene family in pineapple (*Ananas comosus* (L.) Merr.) reveal the role of AcABCG38 in pollen development. *Front. Plant Sci.* **2017**, *8*, 2150. [[CrossRef](#)]
11. Nogia, P.; Pati, P.K. Plant secondary metabolite transporters: Diversity, functionality, and their modulation. *Front. Plant Sci.* **2021**, *12*, 758202. [[CrossRef](#)]
12. Dhara, A.; Raichaudhuri, A. ABCG transporter proteins with beneficial activity on plants. *Phytochemis* **2021**, *184*, 112663. [[CrossRef](#)]
13. Francisco, R.M.; Regalado, A.; Ageorges, A.; Burla, B.J.; Bassin, B.; Eisenach, C.; Zarrouk, O.; Vialet, S.; Marlin, T.; Chaves, M.M.; et al. ABCG1, an ATP binding cassette protein from grape berry, transports anthocyanidin 3-O-Glucosides. *Plant Cell* **2013**, *25*, 1840–1854. [[CrossRef](#)]
14. Demurtas, O.C.; Francisco, R.; Diretto, G.; Ferrante, P.; Frusciante, S.; Pietrella, M.; Aprea, G.; Borghi, L.; Feeney, M.; Frigerio, L.; et al. ABCG transporters mediate the vacuolar accumulation of crocins in *Saffron stigmas*. *Plant Cell* **2019**, *31*, 2789–2804. [[CrossRef](#)]

15. Fu, X.; Liu, H.; Hassani, D.; Peng, B.; Yan, X.; Wang, Y.; Wang, C.; Li, L.; Liu, P.; Pan, Q.; et al. AaABCG40 enhances artemisinin content and modulates drought tolerance in *Artemisia annua*. *Front. Plant Sci.* **2020**, *11*, 950. [[CrossRef](#)]
16. Dahuja, A.; Kumar, R.R.; Sakhare, A.; Watts, A.; Singh, B.; Goswami, S.; Sachdev, A.; Praveen, S. Role of ATP-binding cassette transporters in maintaining plant homeostasis under abiotic and biotic stresses. *Physiol. Plant.* **2021**, *171*, 785–801. [[CrossRef](#)]
17. Khare, D.; Choi, H.; Huh, S.U.; Bassin, B.; Kim, J.; Martinoia, E.; Sohn, K.H.; Paek, K.H.; Lee, Y. *Arabidopsis* ABCG34 contributes to defense against necrotrophic pathogens by mediating the secretion of camalexin. *Proc. Natl. Acad. Sci. USA* **2017**, *114*, 5712–5720. [[CrossRef](#)]
18. Cho, C.H.; Jang, S.; Choi, B.Y.; Hong, D.; Choi, D.S.; Choi, S.; Kim, H.; Han, S.K.; Kim, S.; Kim, M.S.; et al. Phylogenetic analysis of ABCG subfamily proteins in plants: Functional clustering and coevolution with ABCGs of pathogens. *Physiol. Plant.* **2021**, *172*, 1422–1438. [[CrossRef](#)]
19. Bultreys, A.; Trombik, T.; Drozak, A.; Boutry, M. *Nicotiana plumbaginifolia* plants silenced for the ATP-binding cassette transporter gene *NpPDR1* show increased susceptibility to a group of fungal and oomycete pathogens. *Mol. Plant Pathol.* **2009**, *10*, 651–663. [[CrossRef](#)]
20. Stukkens, Y.; Bultreys, A.; Grec, S.; Trombik, T.; Vanham, D.; Boutry, M. *NpPDR1*, a pleiotropic drug resistance-type ATP-binding cassette transporter from *Nicotiana plumbaginifolia*, plays a major role in plant pathogen defense. *Plant Physiol.* **2005**, *139*, 341–352. [[CrossRef](#)]
21. Pierman, B.; Toussaint, F.; Bertin, A.; Lévy, D.; Smargiasso, N.; De Pauw, E.; Boutry, M. Activity of the purified plant ABC transporter NtPDR1 is stimulated by diterpenes and sesquiterpenes involved in constitutive and induced defenses. *J. Biol. Chem.* **2017**, *292*, 19491–19502. [[CrossRef](#)] [[PubMed](#)]
22. Shibata, Y.; Ojika, M.; Sugiyama, A.; Yazaki, K.; Jones, D.A.; Kawakita, K.; Takemtp, D. The full-size ABCG transporters Nb-ABCG1 and Nb-ABCG2 function in pre- and postinvasion defense against *Phytophthora infestans* in *Nicotiana benthamiana*. *The Plant Cell* **2016**, *28*, 1163–1181. [[CrossRef](#)] [[PubMed](#)]
23. Seo, S.; Gomi, K.; Kaku, H.; Abe, H.; Seto, H.; Nakatsu, S.; Neya, M.; Kobayashi, M.; Nakaho, K.; Ichinose, Y. Identification of natural diterpenes that inhibit bacterial wilt disease in tobacco, tomato and *Arabidopsis*. *Plant Cell Physiol.* **2012**, *53*, e1432–e1444. [[CrossRef](#)] [[PubMed](#)]
24. Xu, Z.; Song, N.; Ma, L.; Fang, D.H.; Wu, J.S. NaPDR1 and NaPDR1-like are essential for the resistance of *Nicotiana attenuata* against fungal pathogen *Alternaria alternata*. *Plant Divers.* **2018**, *40*, 68–73. [[CrossRef](#)]
25. Stein, M.; Dittgen, J.; Sanchez-Rodriguez, C.; Hou, B.H.; Molina, A.; Schulze-Lefert, P.; Lipka, V.; Somerville, S. *Arabidopsis* PEN3/PDR8, an ATP binding cassette transporter, contributes to non-host resistance to inappropriate pathogens that enter by direct penetration. *Plant Cell* **2006**, *18*, 731–746. [[CrossRef](#)]
26. Shang, Y.; Xiao, J.; Ma, L.L.; Wang, H.Y.; Qi, Z.J.; Chen, P.D.; Liu, D.J.; Wang, X.E. Characterization of a PDR type ABC transporter gene from wheat (*Triticum aestivum* L.). *Chin. Sci. Bull.* **2009**, *18*, 3249–3257. [[CrossRef](#)]
27. Muhovski, Y.; Jacquemin, J.M.; Batoko, H. Identification and differential induction of ABCG transporter genes in wheat cultivars challenged by a deoxynivalenol-producing *Fusarium graminearum* strain. *Mol. Biol. Rep.* **2014**, *41*, 6181–6194. [[CrossRef](#)]
28. Wang, G.P.; Hou, W.Q.; Zhang, L.; Wu, H.Y.; Zhao, L.F.; Du, X.Y.; Ma, X.; Li, A.F.; Wang, H.W.; Kong, L.R. Functional analysis of a wheat pleiotropic drug resistance gene involved in *Fusarium* head blight resistance. *J. Integr. Agric.* **2016**, *15*, 2215–2227. [[CrossRef](#)]
29. Walter, S.; Kahla, A.; Arunachalam, C.; Perochon, A.; Khan, M.R.; Scofield, S.R.; Doohan, F.M. A wheat ABC transporter contributes to both grain formation and mycotoxin tolerance. *J. Exp. Bot.* **2015**, *66*, 2583–2593. [[CrossRef](#)]
30. Theodoulou, F.L.; Clark, I.M.; He, X.L.; Pallett, K.E.; Cole, D.J.; Hallahan, D.L. Co-induction of glutathione-S-transferases and multidrug resistance associated protein by xenobiotics in wheat. *Pest Manag. Sci.* **2003**, *59*, 202–214. [[CrossRef](#)]
31. Bhati, K.K.; Sharma, S.; Aggarwal, S.; Kaur, M.; Shukla, V.; Kaur, J.; Mantri, S.; Pandey, A.K. Genome-wide identification and expression characterization of ABCC-MRP transporters in hexaploid wheat. *Front. Plant Sci.* **2015**, *6*, 488. [[CrossRef](#)]
32. Wang, X.; Wang, C.; Sheng, H.; Wang, Y.; Zeng, J.; Kang, H.; Fan, X.; Sha, L.; Zhang, H.; Zhou, Y. Transcriptome-wide identification and expression analyses of ABC transporters in dwarf polish wheat under metal stresses. *Biol. Plant.* **2017**, *61*, 293–304. [[CrossRef](#)]
33. Rajagopalan, N.; Lu, Y.; Burton, I.W.; Monteil-Rivera, F.; Halasz, A.; Reimer, E.; Tweidt, R.; Brûlé-Babel, A.; Kutcher, H.R.; You, F.M.; et al. A phenylpropanoid diglyceride associates with the leaf rust resistance *Lr34res* gene in wheat. *Phytochemistry* **2020**, *178*, 112456. [[CrossRef](#)]
34. Sarma, D.; Knott, D.R. The transfer of leaf-rust resistance from *Agropyron* to *Triticum* by irradiation. *Can. J. Genet. Cytol.* **1966**, *8*, 137–143. [[CrossRef](#)]
35. Gupta, S.K.; Charpe, A.; Prabhu, K.V.; Haque, Q.M. Identification and validation of molecular markers linked to the leaf rust resistance gene *Lr19* in wheat. *Theor. Appl. Genet.* **2006**, *113*, 1027–1036. [[CrossRef](#)]
36. Saini, R.G.; Kaur, L. Adult plant leaf rust (*Puccinia recondita tritici*) resistance of known *Lr* genes against three virulence variants of race 77 from Indian sub-continent. *Ind. J. Agric. Res.* **1998**, *68*, 776–779.
37. Prins, R.; Groenewald, J.Z.; Marais, G.F.; Snape, J.W.; Koebner, R.M.D. AFLP and STS tagging of *Lr19*, a gene conferring resistance to leaf rust in wheat. *Theor. Appl. Genet.* **2001**, *103*, 618–624. [[CrossRef](#)]
38. Rai, A.; Singh, A.M.; Ahlawat, A.K.; Kumar, R.R.; Raghunandan, K.; Saini, S.; Ganjewala, D.; Shukla, R.B. Quality evaluation of near isogenic lines of the wheat variety carrying *Sr26*, *Lr19* and *Yr10* genes. *J. Cereal Sci.* **2019**, *88*, 110–117. [[CrossRef](#)]

39. Rosewarne, G.; Bonnett, D.; Rebetzke, G.; Lonergan, P.; Larkin, P. The potential of *Lr19* and *Bdv2* translocations to improve yield and disease resistance in the high rainfall wheat zones of Australia. *Agronomy* **2015**, *5*, 55–70. [[CrossRef](#)]
40. Wang, F.; Yuan, S.T.; Wu, W.Y.; Yang, Y.Q.; Cui, Z.C.; Wang, H.Y.; Liu, D.Q. TaTLP1 interacts with TaPR1 to contribute to wheat defense responses to leaf rust fungus. *PLoS Genet.* **2020**, *16*, e1008713. [[CrossRef](#)]
41. Li, J.Y.; Wang, X.D.; Zhang, L.R.; Meng, Q.F.; Zhang, N.; Yang, W.X.; Liu, D.Q. A wheat NBS-LRR gene TaRGA19 participates in *Lr19*-mediated resistance to *Puccinia triticina*. *Plant Physiol. Bioch.* **2017**, *119*, 1–8.
42. Pourkhorshid, Z.; Dadkhodaie, A.; Shamloo-Dashtpajardi, R. Molecular analyses in wheat and *Aegilops tauschii* reveal a new orthologue of the leaf rust resistance gene *Lr19* on chromosome 7DL of *Ae. tauschii*. *J. Phytopathol.* **2022**, *170*, 255–263. [[CrossRef](#)]
43. Gennaro, A.; Koebner, R.M.D.; Ceoloni, C. A candidate for *Lr19*, an exotic gene conditioning leaf rust resistance in wheat. *Funct. Integr. Genom.* **2009**, *9*, 325–334. [[CrossRef](#)] [[PubMed](#)]
44. Long, D.L.; Kolmer, J.A. A north American system of nomenclature for *Puccinia recondite* f. sp. *tritici*. *Phytopathology* **1989**, *79*, 525–529. [[CrossRef](#)]
45. Lück, S.; Kreszies, T.; Strickert, M.; Schweizer, P.; Kuhlmann, M.; Douchkov, D. siRNA-Finder (si-Fi) software for RNAi-target design and off-target prediction. *Front. Plant Sci.* **2019**, *10*, 1023. [[CrossRef](#)]
46. Zhang, L.R.; Yang, W.X.; Liu, D.Q. *TaRAR1* is required for *Lr24*-mediated wheat leaf rust resistance. *Agric. Sci. China* **2011**, *10*, 1732–1738. [[CrossRef](#)]
47. Wang, X.D.; Wang, X.J.; Deng, L.; Chang, H.T.; Dubcovsky, J.; Feng, H.; Han, Q.M.; Huang, L.L.; Kang, Z.S. Wheat TaNPSN SNARE homologues are involved in vesicle-mediated resistance to stripe rust (*Puccinia striiformis* f. sp. *tritici*). *J. Exp. Bot.* **2014**, *65*, 4807. [[CrossRef](#)]
48. Yan, X.C.; Li, M.M.; Zhang, P.P.; Yin, G.H.; Zhang, H.Z.; Gebrewhid, T.W.; Zhang, J.P.; Dong, L.L.; Liu, D.Q.; Liu, Z.Y.; et al. High-temperature wheat leaf rust resistance gene *Lr13* exhibits pleiotropic effects on hybrid necrosis. *Mol. Plant* **2021**, *14*, 1029–1032. [[CrossRef](#)]
49. Zhao, J.J.; Bi, W.S.; Zhao, S.Q.; Su, J.; Li, M.Y.; Ma, L.S.; Yu, X.M.; Wang, X.D. Wheat apoplast-localized lipid transfer protein *TaLTP3* enhances defense responses against *Puccinia triticina*. *Front. Plant Sci.* **2021**, *12*, 771806. [[CrossRef](#)]
50. Van den Brùle, S.; Muller, A.; Fleming, A.J.; Smart, C.C. The ABC transporter SpTUR2 confers resistance to the antifungal diterpene sclareol. *Plant J.* **2002**, *30*, 649–662. [[CrossRef](#)]
51. Decottignies, A.; Grant, A.M.; Nichols, J.W.; de Wet, H.; McIntosh, D.B.; Goffeau, A. ATPase and multidrug transport activities of the overexpressed yeast ABC protein Yor1p. *J. Biol. Chem.* **1998**, *273*, 12612–12622. [[CrossRef](#)]
52. Campos-Salinas, J.; León-Guerrero, D.; González-Rey, E.; Delgado, M.; Castanys, S.; Pérez-Victoria, J.M.; Gamarro, F. LABCG2, a new ABC transporter implicated in phosphatidylserine exposure, is involved in the infectivity and pathogenicity of *Leishmania*. *PLoS Negl. Trop. Dis.* **2013**, *7*, e2179. [[CrossRef](#)]
53. Deppe, J.P.; Rabbat, R.; Hörtensteiner, S.; Keller, B.; Martinoia, E.; López-Marqués, R.L. The wheat ABC transporter *Lr34* modifies the lipid environment at the plasma membrane. *J. Biol. Chem.* **2018**, *293*, 18667–18679. [[CrossRef](#)]
54. Bai, Z.Y.; Wang, D.M.; Hou, C.Y.; Liu, N.; Han, S.F.; Ma, L.H. Microstructure and ultrastructure infected by wheat rust fungus. *Chin. J. Cell Biol.* **2003**, *25*, 393–397.

Disclaimer/Publisher’s Note: The statements, opinions and data contained in all publications are solely those of the individual author(s) and contributor(s) and not of MDPI and/or the editor(s). MDPI and/or the editor(s) disclaim responsibility for any injury to people or property resulting from any ideas, methods, instructions or products referred to in the content.